J|A|C|S
ARTICLES
Published on Web 01/31/2003

Impact of Multiple Cation−π Interactions upon Calix[4]arene Substrate Binding and Specificity

Alba T. Macias, Joseph E. Norton, and Jeffrey D. Evanseck*

Contribution from the Center for Computational Sciences and Department of Chemistry and Biochemistry, Duquesne University, 600 Forbes Avenue, Pittsburgh, Pennsylvania 15282-1530

Received September 18, 2002; E-mail: evanseck@duq.edu

Abstract: The cation−π interaction influence on the conformation and binding of calix[4]arenes to alkali-metal cations has been studied using a dehydroxylated model. The model allows for the separation of cooperative cation−π and electrostatic forces commonly found in the binding motifs found in calixarene complexes. Starting from the four well-known calix[4]arene conformations, six conformers for this dehydroxylated model (cone, partial cone, flattened cone, chair, 1,2-alternate, and 1,3-alternate) have been characterized by geometry optimization and frequency analysis using the Becke three-parameter exchange functional with the nonlocal correlation functional of Lee, Yang, and Parr and the 6-31G(d) basis set. Without the stabilization provided by the hydroxyl hydrogen bonds in calix[4]arene, neither the cone nor the 1,2-alternate conformation is computed to be a ground-state structure. The partial cone, flattened cone, chair, and 1,3-alternate conformers have been identified as ground-state structures in a vacuum, with the partial cone and the 1,3-alternate as the lowest energy minima in the aromatic model. The C_{4v} cone conformation is found to be a transition structure separating the flattened cone (C_{2v}) conformers. The energetic and structural preferences of the calix[4]arene model change dramatically when it is bound to Li^+, Na^+, and K^+. The number of π-faces, the positioning of these π-faces with respect to the cations, and the nature of the cation were studied as factors in the binding strength. A detailed study of the distances and angles between the aromatic ring centroids and the cations reveals the energetic advantages of multiple weak cation−π interactions. The geometries are often far from the optimal cation−π interaction in which the cation approaches in a perpendicular path the aromatic ring center, where the quadrupole moment is strongest. The results reveal that multiple weaker nonoptimal cation−π interactions contribute significantly to the overall binding strength. This theoretical analysis underscores the importance of neighboring aromatic faces and provides new insight into the significance of cation−π binding, not only for calix[4]arenes, but also for other supramolecular and biological systems.

Introduction

In supramolecular chemistry, a wide variety of macrocyclic receptors are able to form host−guest complexes with neutral, anionic, and cationic species.[1−6] In particular, calix[*n*]arenes have received much attention as a result of their role as biological and synthetic receptor models and easy single-step preparation.[7−10] The flexible calixarene framework requires small energy changes to accommodate guests, which makes them exceptionally resourceful host molecules.[11] Upper and lower rim functionalization of calix[*n*]arenes leading to higher substrate specificity has also contributed to the widespread interest in calix[*n*]arene derivatives.[8] They are known specifically for their applications as ion carriers,[12−15] analytical sensors,[16−19] model structures for biomimetics research,[20−23] and

(1) Lehn, J.-M.; Ball, P. *Supramolecular Chemistry*; Cambridge University Press: Cambridge, 2000.
(2) Lehn, J.-M. *Supramolecular Chemistry/Science. Some Conjectures and Perspectives*; NATO ASI Series, Ser. C; Plenum; New York, 1999; Vol. 527.
(3) Higler, I.; Timmermann, P.; Verboom, W.; Reinhoudt, D. *Eur. J. Org. Chem.* **1947**, *12*, 2689.
(4) Lehn, J.-M. *Supramolecular chemistry: concepts and perspectives: a personal account built upon the George Fisher Baker lectures in chemistry at Cornell University [and the] Lezione Lincee, Accademia nazionale dei Lincei, Roma*; VCH: Weinheim, Germany; New York, 1995.
(5) Raymo, F. M.; Stoddart, J. F. *Chem. Rev.* **1999**, *99*, 1643.
(6) Balzani, V.; Credi, A.; Raymo, F. M.; Stoddart, J. F. *Angew. Chem., Int. Ed.* **2000**, *39*, 3349.
(7) Böhmer, V. *Angew. Chem., Int. Ed. Engl.* **1995**, *34*, 713.
(8) Gutsche, C. D. *Calixarenes Revisited*; The Royal Society of Chemistry: Cambridge, 1998.
(9) Ikeda, A.; Shinkai, S. *Chem. Rev.* **1997**, *97*, 1713.
(10) Ibach, S.; Prautzsch, V.; Vogtle, F.; Chartroux, C.; Gloe, K. *Acc. Chem. Res.* **1999**, *32*, 729.
(11) Casnati, A. *Gazz. Chim. Ital.* **1998**, *127*, 637.
(12) Visser, H. C.; Reinhoudt, D. N.; Dejong, F. *Chem. Soc. Rev.* **1994**, *23*, 75.
(13) van der Veen, N. J.; Egberink, R. J. M.; Engbersen, J. F. J.; van Veggel, F.; Reinhoudt, D. N. *Chem. Commun.* **1999**, 681.
(14) Rudkevich, D. M.; Mercer-Chalmers, J. D.; Verboom, W.; Ungaro, R.; de Jong, F.; Reinhoudt, D. N. *J. Am. Chem. Soc.* **1995**, *117*, 6124.
(15) Kremer, F. J. B.; Chiosis, G.; Engbersen, J. F. J.; Reinhoudt, D. N. *J. Chem. Soc., Perkin Trans. 2* **1994**, 677.
(16) Agrawal, Y. K.; Kunji, S.; Menon, S. K. *Rev. Anal. Chem.* **1998**, *17*, 69.
(17) McQuade, D. T.; Pullen, A. E.; Swager, T. M. *Chem. Rev.* **2000**, *100*, 2537.
(18) Buhlmann, P.; Pretsch, E.; Bakker, E. *Chem. Rev.* **1998**, *98*, 1593.
(19) Diamond, D.; McKervey, M. A. *Chem. Soc. Rev.* **1996**, *23*, 15.
(20) Sénèque, O.; Rager, M.-N.; Giorgi, M.; Reinaud, O. *J. Am. Chem. Soc.* **2000**, *122*, 6183.
(21) Molenveld, P.; Engbersen, J. F. J.; Kooijman, H.; Spek, A. L.; Reinhoudt, D. N. *J. Am. Chem. Soc.* **1998**, *120*, 6726.
(22) Caselli, A.; Solari, E.; Scopelliti, R.; Floriani, C.; Re, N.; Rizzoli, C.; Chiesi-Villa, A. *J. Am. Chem. Soc.* **2000**, *122*, 3652.
(23) Steed, J. W.; Juneja, R. K.; Burkhalter, R. S.; Atwood, J. L. *Chem. Commun.* **1994**, 2205.

tools for studying the stabilizing effects of intramolecular and intermolecular hydrogen bonding.[24−30]

The four main conformations of calix[4]arenes have been identified by Gutsche as cone, partial cone, 1,2-alternate, and 1,3-alternate.[25] The conformational stability of substituted calix[4]arenes has been mainly attributed to hydrogen bonding, steric and electrostatic forces, guest complexation, and to a lesser degree solvent effects.[7−10,28,31,32] The different calixarene conformations can be achieved by appropriate functionalization.[33−35] When the substituents in the lower rim are small and allow the phenyl rings to flip, the different conformations exist in equilibrium at room temperature. Transitions between conformers of a variety of calix[4]arenes have been previously reported.[26,36−45] Hydrogen bonding among the four hydroxyl groups of **2** and **3** stabilize the cone, which is the most stable conformer in both the gas and aqueous phases according to experimental[24−26] and theoretical[36,37,41,46−49] studies. Experimental studies of partially methylated *tert*-butylcalix[4]arenes **4**−**6** emphasize the role of hydrogen bonding in determining the conformational distribution and stability. Although the methyl ethers allow phenyl rotation and have conformational inversion barriers similar to that of **2**,[50] the number of conformations in equilibrium is reduced when hydroxyls are replaced by methyl ethers. The 1,2-dimethyl ether **4** adopts only the cone and partial cone conformations,[31] and the 1,3-dimethyl ether **5** is detected only in the cone conformation.[31,51] When there is no hydrogen bonding, the partial cone becomes the most stable conformer for tetra-O-methylated calix[4]arene **6**.[36] Without hydrogen bond stabilization, as in **1**, there is a greater role for other forces in the determination of conformational equilibrium. The great variety of substituents used in calixarene chemistry introduces a complex mixture of inter- and intramolecular forces, which ultimately determines the conformational distribution.

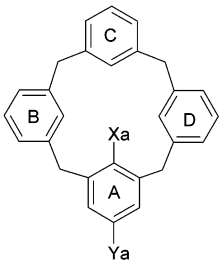

1	X_{a-d} = H	Y_{a-d} = H	
2	X_{a-d} = OH	Y_{a-d} = H	
3	X_{a-d} = OH	Y_{a-d} = t-Bu	
4	$X_{a,b}$ = OH	$X_{c,d}$ = OCH_3	Y_{a-d} = t-Bu
5	$X_{a,c}$ = OH	$X_{b,d}$ = OCH_3	Y_{a-d} = t-Bu
6	X_{a-d} = OCH_3	Y_{a-d} = t-Bu	
7	X_{a-d} = OCH_3	Y_{a-d} = H	

Recently, calixarene applications as ionophores for cations have underscored the importance of the cation−π interaction in supramolecular complexation.[52−54] The cation−π interaction[55] is a strong noncovalent interaction present in both biochemical[56−65] and supramolecular systems.[9,52,66,67] Crystal structures, ^{1}H NMR spectroscopy, and mass spectrometry provide evidence for the presence of cation−π interactions in calixarenes, which has been previously reviewed.[52] The cation−π interaction strength was first revealed in 1981 by Kebarly and co-workers when gas-phase equilibrium studies showed that the binding between K^+ and benzene could compete with the interaction between K^+ and water.[68] Over the following decade, computational research on the cation−π interaction was extensive as reported in the review by Ma and Dougherty.[55] Over the last few years, studies have focused on the energetics of the aromatic interaction with metal[69−80] and ammonium[81−83] cations, as well

(24) Gutsche, C. D. *Acc. Chem. Res.* **1983**, *16*, 161.
(25) Gutsche, C. D.; Bauer, L. J. *J. Am. Chem. Soc.* **1985**, *107*, 6052.
(26) Araki, K.; Shinkai, S.; Matsuda, T. *Chem. Lett.* **1989**, 581.
(27) Grynszpan, F.; Goren, Z.; Biali, S. E. *J. Org. Chem.* **1991**, *56*, 532.
(28) Rudkevich, D. M. *Eur. J. Chem.* **2000**, *6*, 2679.
(29) Conn, M. M.; Rebek, J. *Chem. Rev.* **1997**, *97*, 1647.
(30) Frkanec, L.; Visnjevac, A.; Kojic-Prodic, B.; Zinic, M. *Chem.−Eur. J.* **2000**, *6*, 442.
(31) Groenen, L. C.; Steinwender, E.; Lutz, B. T. G.; Vandermaas, J. H.; Reinhoudt, D. N. *J. Chem. Soc., Perkin Trans. 2* **1992**, 1893.
(32) Iwamoto, K.; Ikeda, A.; Araki, K.; Harada, T.; Shinkai, S. *Tetrahedron* **1993**, *49*, 9937.
(33) Gutsche, C. D.; Reddy, P. A. *J. Org. Chem.* **1991**, *56*, 4783.
(34) Verboom, W.; Datta, S.; Asfari, Z.; Harkema, S.; Reinhoudt, D. N. *J. Org. Chem.* **1992**, *57*, 5394.
(35) Iwamoto, K.; Araki, K.; Shinkai, S. *J. Org. Chem.* **1991**, *56*, 4955.
(36) Harada, T.; Rudzinski, J. M.; Shinkai, S. *J. Chem. Soc., Perkin Trans. 2* **1992**, 2109.
(37) Harada, T.; Ohseto, F.; Shinkai, S. *Tetrahedron* **1994**, *50*, 13377.
(38) Araki, K.; Inada, K.; Otsuka, H.; Shinkai, S. *Tetrahedron* **1993**, *49*, 9465.
(39) Biali, S. E.; Böhmer, V.; Cohen, S.; Ferguson, G.; Gruttner, C.; Grynszpan, F.; Paulus, E. F.; Thondorf, I.; Vogt, W. *J. Am. Chem. Soc.* **1996**, *118*, 12938.
(40) Biali, S. E.; Böhmer, V.; Brenn, J.; Frings, M.; Thondorf, I.; Vogt, W.; Wohnert, J. *J. Org. Chem.* **1997**, *62*, 8350.
(41) Fischer, S.; Grootenhuis, P. D. J.; Groenen, L. C.; Vanhoorn, W. P.; Vanveggel, F.; Reinhoudt, D. N.; Karplus, M. *J. Am. Chem. Soc.* **1995**, *117*, 1611.
(42) Grynszpan, F.; Biali, S. E. *Tetrahedron Lett.* **1991**, *32*, 5155.
(43) Thondorf, I.; Brenn, J.; Brandt, W.; Böhmer, V. *Tetrahedron Lett.* **1995**, *36*, 6665.
(44) VanGelder, J. M.; Brenn, J.; Thondorf, I.; Biali, S. E. *J. Org. Chem.* **1997**, *62*, 3511.
(45) Thondorf, I. *J. Chem. Soc., Perkin Trans. 2* **1999**, 1791.
(46) Bernardino, R. J.; Cabral, B. J. C. *J. Phys. Chem. A* **1999**, *103*, 9080.
(47) Harada, T.; Shinkai, S. *J. Chem. Soc., Perkin Trans. 2* **1995**, 2231.
(48) Lipkowitz, K. B.; Pearl, G. *J. Org. Chem.* **1993**, *58*, 6729.
(49) Grootenhuis, P. D. J.; Kollman, P. A.; Groenen, L. C.; Reinhoudt, D. N.; Vanhummel, G. J.; Ugozzoli, F.; Andreetti, G. D. *J. Am. Chem. Soc.* **1990**, *112*, 4165.
(50) Gutsche, C. D.; Dhawan, B.; Levine, J. A.; No, K. H.; Bauer, L. J. *Tetrahedron* **1983**, *39*, 409.
(51) Alfieri, C.; Dradi, E.; Pochini, A.; Ungaro, R. *Gazz. Chim. Ital.* **1989**, *119*, 335.
(52) Lhotak, P.; Shinkai, S. *J. Phys. Org. Chem.* **1997**, *10*, 273.
(53) Arnecke, R.; Böhmer, V.; Cacciapaglia, R.; Cort, A. D.; Mandolini, L. *Tetrahedron* **1997**, *53*, 4901.
(54) Matthews, S. E.; Schmitt, P.; Felix, V.; Drew, M. G. B.; Beer, P. D. *J. Am. Chem. Soc.* **2002**, *124*, 1341.
(55) Ma, J. C.; Dougherty, D. A. *Chem. Rev.* **1997**, *97*, 1303.
(56) Burley, S. K.; Petsko, G. A. *FEBS Lett.* **1986**, *203*, 13.
(57) Dougherty, D. A. *Science* **1996**, *271*, 163.
(58) Scrutton, N. S.; Raine, A. R. C. *Biochem. J.* **1996**, *319*, 1.
(59) Gallivan, J. P.; Dougherty, D. A. *Proc. Natl. Acad. Sci. U.S.A.* **1999**, *96*, 9459.
(60) Minoux, H.; Chipot, C. *J. Am. Chem. Soc.* **1999**, *121*, 10366.
(61) Burghardt, T. P.; Juranic, N.; Macura, S.; Ajtai, K. *Biopolymers* **2002**, *63*, 261.
(62) Shi, Z. S.; Olson, C. A.; Kallenbach, N. R. *J. Am. Chem. Soc.* **2002**, *124*, 3284.
(63) Orner, B. P.; Salvatella, X.; Quesada, J. S.; de Mendoza, J.; Giralt, E.; Hamilton, A. D. *Angew. Chem., Int. Ed.* **2002**, *41*, 117.
(64) Howerton, S. B.; Sines, C. C.; VanDerveer, D.; Williams, L. D. *Biochemistry* **2001**, *40*, 10023.
(65) Zacharias, N.; Dougherty, D. A. *Trends Pharmacol. Sci.* **2002**, *23*, 281.
(66) Gokel, G. W.; De Wall, S. L.; Meadows, E. S. *Eur. J. Org. Chem.* **2000**, 2967.
(67) Gokel, G. W.; Barbour, L. J.; De Wall, S. L.; Meadows, E. S. *Coord. Chem. Rev.* **2001**, *222*, 127.
(68) Sunner, J.; Nishizawa, K.; Kebarly, P. *J. Phys. Chem.* **1981**, *85*, 1814.
(69) Feller, D.; Dixon, D. A.; Nicholas, J. B. *J. Phys. Chem. A* **2000**, *104*, 11414.
(70) Feller, D. *Chem. Phys. Lett.* **2000**, *322*, 543.
(71) Nicholas, J. B.; Hay, B. P.; Dixon, D. A. *J. Phys. Chem. A* **1999**, *103*, 1394.
(72) Nicholas, J. B.; Hay, B. P. *J. Phys. Chem. A* **1999**, *103*, 9815.
(73) Choi, H. S.; Suh, S. B.; Cho, S. J.; Kim, K. S. *Proc. Natl. Acad. Sci. U.S.A.* **1998**, *95*, 12094.
(74) McMahon, T. B.; Ohanessian, G. *Chem.−Eur. J.* **2000**, *6*, 2931.
(75) Amicangelo, J. C.; Armentrout, P. B. *J. Phys. Chem. A* **2000**, *104*, 11420.
(76) Armentrout, P. B.; Rodgers, M. T. *J. Phys. Chem. A* **2000**, *104*, 2238.
(77) Ikuta, S. *J. Mol. Struct.: THEOCHEM* **2000**, *530*, 201.
(78) Hoyau, S.; Norrman, K.; McMahon, T. B.; Ohanessian, G. *J. Am. Chem. Soc.* **1999**, *121*, 8864.
(79) Donini, O.; Weaver, D. F. *J. Comput. Chem.* **1998**, *19*, 1515.
(80) Gapeev, A.; Dunbar, R. C. *J. Am. Chem. Soc.* **2001**, *123*, 8360.
(81) Deakyne, C. A.; Meot-Ner, M. *J. Am. Chem. Soc.* **1999**, *121*, 1546.
(82) Felder, C.; Jiang, H. L.; Zhu, W. L.; Chen, K. X.; Silman, I.; Botti, S. A.; Sussman, J. L. *J. Phys. Chem. A* **2001**, *105*, 1326.
(83) Inoue, Y.; Sugio, S.; Andzelm, J.; Nakamura, N. *J. Phys. Chem. A* **1998**, *102*, 646.

as on the nature of the interaction itself.[84−91] A detailed review by Feller and co-workers on recent experimental and computational advances concerning alkali-metal cation and benzene complexation has been published.[69] The cation−π interaction between benzene and alkali-metal cations has been computed with high levels of theory,[69−72,75,76] with the majority of results in agreement with recent gas-phase experimental data.[75,76]

The binding modes of calixarene−cation systems are known to involve cooperative effects between cation−π and electrostatic forces.[52] Theoretical studies of anisole, a model for the calixarene moiety phenyl−O−CH_2X, reveal that alkali-metal cations (except Li^+) prefer to bind to the oxygen rather than to the phenyl by approximately 1 kcal/mol.[72] The high complexity of host−guest interactions in calixarenes was illustrated by theoretical studies on the binding of Na^+ and Cs^+ to conformers of tetramethoxycalix[4]arene, **7**.[92] In several conformations, **7** formed stronger complexes when more cation−π interactions with the cations were possible. In a recent theoretical study of calix[4]arene **2**, Li^+ and Na^+ bound closely to the oxygens while K^+, Cs^+, and Rb^+ bound within the aromatic cavity of the cone conformation.[93] Due to the nature of calixarene complexes previously reported, little is known concerning the influence of cation−π interactions upon conformational stability and selective binding of ligands cleanly separated from electrostatic and hydrogen-bonding effects.

Experimental evidence suggests a role for multiple cation−π interactions in biological and supramolecular systems. While the binding strength of most single noncovalent bonds is relatively weak (∼2−6 kcal/mol) in aqueous environments, multiple bonds increase the total binding strength and selectivity.[94] Macrocyclic hosts synthesized to investigate the cation−π interaction by Dougherty and co-workers contained multiple aromatic binding sites.[55] In biological systems, there are cationic binding sites rich in aromatic amino acids; for example, phosphocholine-binding immunoglobulin Fab McPC603,[95] phosphatidylcholine transfer protein,[96] and the complex between methylated histone and heterochromatin-associated protein 1[97,98] have three aromatic residues that interact with the substrate. ^{1}H NMR binding studies reveal that the presence of additional double bonds in vinyl-substituted calixarene derivatives enhances the binding of cations, suggesting that additional cation−π interactions improve complexation.[99] The X-ray structure of the synthetic receptor resorcin[4]arene complexed with acetylcholine trimethylammonium reveals the presence of multiple cation−π interactions,[100] since the three methyl groups are in close contact (<3.8 Å) with the aromatic ring centroids. Consequently, the calixarene aromatic core provides an excellent model for studying the relationship between binding strength and the number and geometry of cation−π interactions, since the different conformations provide a variety of aromatic binding motifs.

A majority of computational studies on calixarene conformations and binding of ligands have been reported using molecular mechanical force fields. The conformations of **1**[27,37,101,102] and partially dehydroxylated calix[4]arenes[27,45,101,102] have been studied by molecular mechanical methods using the MM2 and MM3(92) force fields.[103] The cone conformation is found to be the most stable in the majority of cases, but the results disagree depending upon the force field used. An X-ray structure of **1** did not clarify which conformer is more stable, since it reveals a chairlike conformation, which is attributed to favorable packing in the crystal and not to the stability of the molecule's conformation.[101] The large computational resources required to evaluate the energy and structure of calix[*n*]arenes have prevented extensive ab initio and density functional treatments until recently. Improvements in computers and parallel algorithms allow calculations on these large systems. Recently, density functional studies on hydroxylated calix[4]arene,[46,93] thiacalix[4]arene,[104] and tetramethoxycalix[4]arene[92] have been published. However, a full density functional assessment of the aromatic core focusing on the effects of cation−π interactions, void of competing forces (such as hydrogen bonding), upon the conformation and ligand binding has not been presented to date.

To clarify the role of the aromatic core and cation−π interactions in determining the conformations and energies of calix[4]arenes and their complexes, we have undertaken a density functional study of a dehydroxylated calix[4]arene model (**1**) with alkali-metal cations Li^+, Na^+, and K^+. The flexibility and lack of substituents in **1** can provide a better understanding of the cation−π interaction strength and induced structural variations of biochemical and supramolecular systems. The computations provide deeper insight into the nature of the cation−π interactions in the absence of competing forces and supplement a more complete understanding of the experimental binding of calix[4]arenes, in which electrostatic interactions and solvent effects are well-known.

Computational Methods

All density functional theory (DFT) calculations were carried out using the Gaussian 98 program[105] using an IBM 16-node RS/6000 SP.[106] The level of theory used was Becke's three-parameter exchange

(84) Caldwell, J. W.; Kollman, P. A. *J. Am. Chem. Soc.* **1995**, *117*, 4177.
(85) Tsuzuki, S.; Yoshida, M.; Uchimaru, T.; Mikami, M. *J. Phys. Chem. A* **2001**, *105*, 769.
(86) Cubero, E.; Luque, F. J.; Orozco, M. *Proc. Natl. Acad. Sci. U.S.A.* **1998**, *95*, 5976.
(87) Cubero, E.; Orozco, M.; Luque, F. J. *J. Phys. Chem. A* **1999**, *103*, 315.
(88) Mo, Y. R.; Subramanian, G.; Gao, J. L.; Ferguson, D. M. *J. Am. Chem. Soc.* **2002**, *124*, 4832.
(89) Bartoli, S.; Roelens, S. *J. Am. Chem. Soc.* **2002**, *124*, 8307.
(90) Aschi, M.; Mazza, F.; Di Nola, A. *J. Mol. Struct.: THEOCHEM* **2002**, *587*, 177.
(91) Fukin, G. K.; Linderman, S. V.; Kochi, J. K. *J. Am. Chem. Soc.* **2002**, *124*, 8329.
(92) Hay, B. P.; Nicholas, J. B.; Feller, D. *J. Am. Chem. Soc.* **2000**, *122*, 10083.
(93) Bernardino, R. J.; Cabral, B. J. C. *Supramol. Chem.* **2002**, *14*, 57.
(94) Muller-Dethlefs, K.; Hobza, P. *Chem. Rev.* **2000**, *100*, 143.
(95) Dougherty, D. A.; Stauffer, D. A. *Science* **1990**, *250*, 1558.
(96) Roderick, S. L.; Chan, W. W.; Agate, D. S.; Olsen, L. R.; Vetting, M. W.; Rajashankar, K. R.; Cohen, D. E. *Nat. Struct. Biol.* **2002**, *9*, 507.
(97) Nielsen, P. R.; Nietlispach, D.; Mott, H. R.; Callaghan, J. M.; Bannister, A.; Kouzarides, T.; Murzin, A. G.; Murzina, N. V.; Laue, E. D. *Nature* **2002**, *416*, 103.
(98) Jacobs, S. A.; Khorasanizadeh, S. *Science* **2002**, *295*, 2080.
(99) Lhotak, P.; Nakamura, R.; Shinkai, S. *Supramol. Chem.* **1997**, *8*, 333.
(100) Murayama, K.; Aoki, K. *Chem. Commun.* **1997**, 119.
(101) McMurry, J. E.; Phelan, J. C. *Tetrahedron Lett.* **1991**, *32*, 5655.
(102) Fukazawa, Y.; Deyama, K.; Usui, S. *Tetrahedron Lett.* **1992**, *33*, 5803.
(103) Allinger, N. L.; Yuh, Y. H.; Lii, J. H. *J. Am. Chem. Soc.* **1989**, *111*, 8551.
(104) Bemardino, R. J.; Cabral, B. J. C. *J. Mol. Struct.: THEOCHEM* **2001**, *549*, 253.
(105) Frisch, M. J.; Trucks, G. W.; Schlegel, H. B.; Scuseria, G. E.; Robb, M. A.; Cheeseman, J. R.; Zakrzewski, V. G.; Montgomery, J. A., Jr.; Stratmann, R. E.; Burant, J. C.; Dapprich, S.; Millam, J. M.; Daniels, A. D.; Kudin, K. N.; Strain, M. C.; Farkas, O.; Tomasi, J.; Barone, V.; Cossi, M.; Cammi, R.; Mennucci, B.; Pomelli, C.; Adamo, C.; Clifford, S.; Ochterski, J.; Petersson, G. A.; Ayala, P. Y.; Cui, Q.; Morokuma, K.; Malick, D. K.; Rabuck, A. D.; Raghavachari, K.; Foresman, J. B.; Cioslowski, J.; Ortiz, J. V.; Stefanov, B. B.; Liu, G.; Liashenko, A.; Piskorz, P.; Komaromi, I.; Gomperts, R.; Martin, R. L.; Fox, D. J.; Keith, T.; Al-Laham, M. A.; Peng, C. Y.; Nanayakkara, A.; Gonzalez, C.; Challacombe, M.; Gill, P. M. W.; Johnson, B.; Chen, W.; Wong, M. W.; Andres, J. L.; Gonzalez, C.; Head-Gordon, M.; Replogle, E. S.; Pople, J. A. *Gaussian 98*, Revision A.3; Gaussian, Inc.: Pittsburgh, PA, 1998.
(106) Thanks to IBM's commitment to underrepresented student research and education, and for the SUR grant for computer equipment.

Table 1. Accuracy of B3LYP/6-31G(d) in the Computation of Cation−π Interaction Energies[a]

		ΔE^b	$\Delta E^{b,cp}$	$\Delta E_0^{b,cp\,b}$	ΔH_T^b	$\Delta H_T^{b,cp}$	CP
Ben−Li^+	CID[c]			−38.5 ± 3.2	−39.3 ± 3.2 (T = 298)		
	ICR[d]				−37.9 (T = 298)		
	B3LYP/6-31G(d)[e]	−42.4	−40.3	−38.6	−41.3 (T = 298)	−39.2	2.1
	MP2/6-311+G(d)[f]	−40.2	−36.0		−39.2 (T = 298)	−35.0	4.2
	MP2(TZ/DZ)[c,g]			−34.2			2.3
	CCSDT+CV[h]	−38.0 ± 0.2			−36.8 ± 0.2 (T = 298)		
Ben−Na^+	CID[c]			−22.1 ± 1.4	−22.5 ± 1.5 (T = 298)		
	CID[i]				−21.4 ± 1.0 (T = 298)		
	HPMS[j]				−28.0 ± 1.5 (T = 610)		
	CCID[k]			−22.8 ± 1.4	−23.2 ± 1.4 (T = 298)		
	B3LYP/6-31G(d)[e]	−28.5	−26.7	−25.8	−27.8 (T = 298)	−26.0	1.8
	MP2/6-311+G(d)[f]	−24.9	−21.9		−24.0 (T = 610)	−21.0	3.0
	MP2(TZ/DZ)[c,g,l]			−21.4			2.3
	B3LYP(TZ/DZ)[i,m]			−22.7			
	CCSDT+CV[h]	−25.4 ± 0.3			−24.7 ± 0.3 (T = 298)		
Ben−K^+	CID[c]			−17.5 ± 1.0	−17.7 ± 1.0 (T = 298)		
	HPMS[n]				−18.3[o] (T = 500)		
	B3LYP/6-31G(d)[e]	−18.7	−16.8	−16.1	−18.1 (T = 298)	−16.2	1.9
	MP2/6-311+G(d)[f]	−18.5	−16.7		−17.8 (T = 500)	−16.0	1.8
	MP2(TZ/DZ)[c,g]			−17.1			1.3
	CCSDT+CV[h]	−20.6 ± 0.4			−20.1 ± 0.4 (T = 298)		
Ben−Li^+−Ben	CID[c]			−63.4 ± 4.8	−64.1 ± 4.9 (T = 298)		
	B3LYP/6-31G(d)[p]	−69.7	−66.5	−64.0	−67.8 (T = 298)	−64.6	3.2
	MP2(TZ/DZ)[c,g]			−60.1			6.9
Ben−Na^+−Ben	CID[c]			−41.2 ± 2.8	−41.7 ± 2.8 (T = 298)		
	B3LYP/6-31G(d)[p]	−51.2	−47.8	−46.1	−49.6 (T = 298)	−46.2	3.4
	MP2(TZ/DZ)[c,g]			−38.5			6.2
Ben−K^+−Ben	CID[c]			−33.6 ± 2.5	−34.0 ± 2.7 (T = 298)		
	HPMS[n]				−35.5 (T = 500)		
	B3LYP/6-31G(d)[p]	−35.3	−31.6	−30.2	−33.4 (T = 298)	−29.7	3.7
	MP2(TZ/DZ)[c,g]			−30.5			3.6

[a] Energies and enthalpies are reported in kilocalories per mole. T values are given in Kelvin. Ben = benzene. [b] Only computed values are CP corrected. [c] Reference 75 using a double octopole apparatus. [d] Reference 115. [e] Present results, computed with C_{6v}, Cat−R_Y distances were 1.879, 2.376, and 2.892 Å for Li^+, Na^+, and K^+, respectively. [f] Reference 71. [g] MP2(full)/6-311+G(2d,2p)//MP2(full)/6-31G(d). [h] Reference 69. [i] Reference 76 using a single octopole apparatus. [j] Reference 113. [k] Reference 114. [l] Reference 78. [m] B3LYP/6-311+G(2d,2p)//B3LYP/6-31G(d). [n] Reference 68, [o] Experimental correction for molecular dissociation. [p] Present results, computed with D_{6h}. Na^+ and Li^+ 2:1 complexes with D_{6h} symmetry gave small imaginary frequencies due to hydrogen repulsion. After the rings were rotated, a true minimum was obtained, and the ΔE^b values remained within 0.1 kcal of the D_{6h} value.

functional in combination with the nonlocal correlation functional of Lee, Yang, and Parr[107] (B3LYP) and the 6-31G(d) basis set.[108,109] The 6-31G(d) basis set has been shown to reproduce experimental binding enthalpies (ΔH^b) of the cation−π interaction between benzene and alkali-metal cations.[55,110−112] This basis set reproduces the experimental data even better than more complete basis sets,[71] probably due to a fortuitous cancellation of errors when coupled with limited chemical methods. The different conformers of **1** and the complexes of these conformers with the Li^+, Na^+, and K^+ cations were geometry optimized. Vibrational frequency analysis was used to confirm whether the stationary points were minima or transition structures, and provided the zero-point energy (ZPE) and thermodynamic corrections necessary to obtain the enthalpy (ΔH) and Gibbs free energy (ΔG) at 298 K.

The B3LYP density functional method was chosen for this study due to its excellent agreement (Table 1) with experimental binding enthalpies at 298 K for benzene interacting with Li^+ and K^+ from collision-induced dissociation with guided ion beam mass spectrometry (CID)[75] and for benzene interacting with Na^+ and K^+ from equilibrium high-pressure mass spectrometry (HPMS).[113] One problematic point has been with understanding the binding of Na^+ with benzene. There are four available experimental measurements of the enthalpy of binding between Na^+ and benzene spanning over a 6 kcal/mol range. HPMS[113] results in $\Delta H_{610} = -28.0 \pm 1.5$ kcal/mol, whereas CID[76] gives $\Delta H_{298} = -21.4 \pm 1.0$ kcal/mol. The two values lie outside their respective experimental uncertainties. The most recent competitive CID (CCID)[114] results in a stronger binding with $\Delta H_{298} = -23.2 \pm 1.4$ and $\Delta G_{298} = -15.9 \pm 1.8$ kcal/mol, which is in agreement with a Fourier transform ion cyclotron resonance (FTICR) experiment[74] in which $\Delta G_{298} = -15.7 \pm 0.3$ kcal/mol. High-level theoretical studies are also inconsistent. Computed second-order Møller−Plesset (MP2)[71,76,78] and G3 and CBS-4[76] values for the binding between Na^+ and benzene are in agreement with the lower CID values, while a study that extrapolates to the complete basis set (CBS) limit with core/valence and higher order correlation effects, CCSD(T) + CV with $\Delta H_{298} = -24.7 \pm 0.3$, is in agreement with the CCID value.[69] Consequently, the discrepancy between values for Na^+ and benzene bonding remains unclear. For this study, the energies computed using B3LYP/6-31G(d) are solidly within reported experimental errors for the enthalpy of binding between benzene and Li^+ and K^+. Our computations are consistent with the experimental HPMS enthalpy of binding for Na^+−benzene, yet outside the CID experimental and computational uncertainty of other reports. Nevertheless, the currently unresolved issue of Na^+ binding with benzene is not the focus of this paper, nor does it change the interpretations and conclusions.

B3LYP/6-31G(d)'s agreement with experiment and its computational efficiency make it the method of choice for this study on a large aromatic model, allowing the calculation of frequencies for the identification of stable structures, which is one of the main goals and could not be done with higher levels of theory such as MP2. Recent

(107) Lee, C.; Yang, W.; Parr, R. G. *Phys. Rev.* **1988**, *37*, 785.
(108) Francl, M. M.; Petro, W. J.; Hehre, W. J.; Binkley, J. S.; Gordon, M. S.; DeFree, D. J.; Pople, J. A. *J. Chem. Phys.* **1982**, *77*, 3654.
(109) Rassolov, V.; Pople, J. A.; Ratner, M.; Windus, T. L. *J. Chem. Phys.* **1998**, *109*, 1223.
(110) Gallivan, J. P.; Dougherty, D. A. *J. Am. Chem. Soc.* **2000**, *122*, 870.
(111) Mecozzi, S.; West, A. P.; Dougherty, D. A. *Proc. Natl. Acad. Sci. U.S.A.* **1996**, *93*, 10566.
(112) Mecozzi, S.; West, A. P.; Dougherty, D. A. *J. Am. Chem. Soc.* **1996**, *118*, 2307.
(113) Guo, B. C.; Purnell, J. W.; Castleman, A. W. J. *Chem. Phys. Lett.* **1990**, *168*, 155.
(114) Amicangelo, J. C.; Armentrout, P. B. *Int. J. Mass Spectrom.* **2001**, *212*, 301.

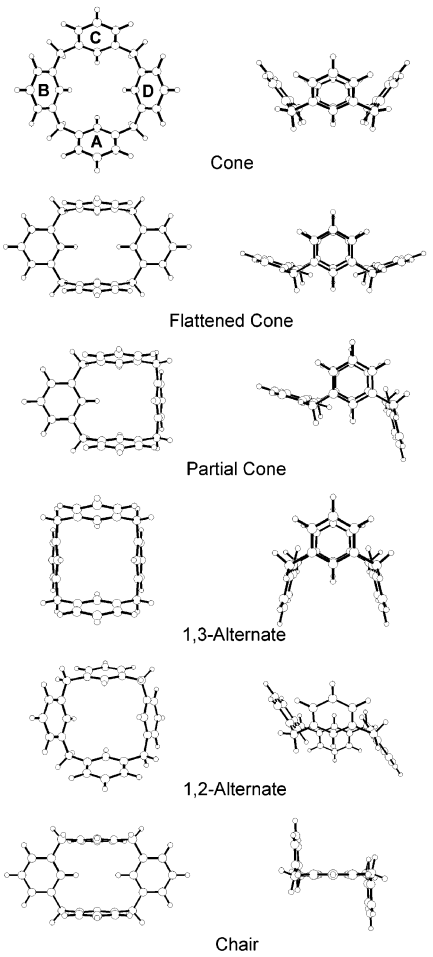

Figure 1. Two perspectives of the geometry-optimized B3LYP/6-31G(d) conformers of **1**.

studies have raised concerns about the lack of dispersion energy in DFT methods. Comparisons between DFT and MP2 reveal differences in the conformational stability of **7** of 1 kcal/mol[92] and differences in binding in other systems of 1−2 kcal/mol.[78,116] However, Table 1 shows that such differences are not uncommon even with methods that take dispersion into account. Caution should be exercised when drawing conclusions; however, the known limitation of DFT is not a significant factor in this study. The computed electronic binding energies (ΔE^b) are also in excellent agreement with the experimental binding enthalpies (ΔH_T^b). Consequently, ΔE^b will be discussed throughout this study. Inclusion of all corrections to the binding energies does not change a conformer's cation binding selectivity. Binding energies were calculated by subtracting the energies of the monomers from the energies of the complexes of those monomers. Basis set superimposition error (BSSE) was not included, except for a few illustrative examples, which were calculated by the counterpoise (CP) correction method,[117] as discussed in more detail in the next section.

Results and Discussion

Energetic Stability of Conformers. The geometries of the six optimized conformers of structure **1** are shown in Figure 1. The four well-known conformations of calix[4]arene identified by Gutsche (cone, partial cone, 1,2-alternate, and 1,3-alternate) were located using symmetry constraints. While the C_{2v} 1,3-alternate and C_s partial cone conformers are predicted to exist in the gas phase, the C_{4v} cone and the D_{2d} 1,2-alternate are not true minima in a vacuum. Vibrational analysis on the optimized C_{4v} cone gave an imaginary frequency of -17 cm^{-1} corresponding to a deformation in which the two opposing rings move closer to each other while the other two move further apart. The complex was reoptimized with tighter SCF convergence criteria of 10^{-9} and disabled symmetry instead of 10^{-8}. The same energy and imaginary frequency were obtained. The cone symmetry was then lowered to C_{2v}, and a fifth conformer was optimized which lacked imaginary frequencies. This C_{2v} cone corresponds to the flattened cone, which was previously identified and is sometimes referred to as the pinched cone.[36,49] Despite extensive searches, a stable 1,2-alternate conformation could not be located. Two strong imaginary frequencies were computed, where the adjacent rings tried to minimize their repulsion. A sixth conformer, the chair, was optimized without any symmetry restrictions, and frequency analysis established it as a minimum. The chair corresponds to the geometry obtained in a previous study where the X-ray crystal structure was minimized with molecular mechanics.[101]

According to the B3LYP/6-31G(d) electronic energies (E) in Table 2, the order of the conformers in decreasing stability and the electronic energy difference among conformers (ΔE, kcal/mol) is partial cone (0.0), 1,3-alternate (0.21), flattened cone (0.47), and chair (0.65). The C_{4v} cone corresponds to the transition structures between flattened C_{2v} cones, with a barrier height of 0.43 kcal/mol. The energy differences among the lowest four conformers are insignificant at room temperature, and the possibility exists that the energetic order could be subject to thermal corrections and dispersion forces. Basis set effects were explored by computing energies with a more complete basis set (B3LYP/6-311+G(2d,2p)). This caused a decrease in the energy differences among conformers, as compared to the results from the smaller basis set, reaffirming that a definite assignment of a global minimum is not possible. Thermodynamic energy corrections do not reorder the energetic ranking of the conformers, but do change their relative values, as seen by the ΔH values in Table 2. Entropy shuffles the ordering of the conformers, which are separated by less than 0.1 kcal/mol. According to differential Gibbs energy differences (ΔG, kcal/mol), the order starting with the most stable is 1,3-alternate (0.0), partial cone (0.10), chair (0.95), and flattened cone (0.96). The largest change is that the activation free energy barrier increases to 3.9 kcal/mol for the C_{4v} cone. A definite assignment of the global minimum is not possible, due to the small energy differences of the conformational distribution, but most importantly, it is not the cone as previously thought.

(a) Cone and Flattened Cone. It is clear from the DFT calculations that the C_{4v} cone conformation is a transition structure. The present results contradict previously reported gas-phase molecular mechanics studies,[37,101] where the MM2 and MM3(92) force fields predict that the C_{4v} cone of **1** is the most stable conformer. Our results demonstrate the importance of hydrogen bonding in the stability of the cone in **2**, since without hydroxyls **1** is predicted not to exist as a cone in the gas phase. To compare directly cones **1** and **2**, we repeated the optimization of cone **2** which had been previously reported,[46] but for the first time with a vibrational frequency analysis including electron

(115) Woodin, R. L.; Beauchamp, J. L. *J. Am. Chem. Soc.* **1978**, *100*, 501.
(116) Liu, T.; Gu, J. D.; Tan, X. J.; Zhu, W. L.; Luo, X. M.; Jiang, H. L.; Ji, R. Y.; Chen, K. X.; Silman, I.; Sussman, J. L. *J. Phys. Chem. A* **2001**, *105*, 5431.
(117) Duijneveldt, F. B.; Duijneveldt-van de Rijdt, J. G. C. M.; Lenthe, J. H. *Chem. Rev.* **1994**, *94*, 1873.

Table 2. Calculated Energy Differences of the Aromatic Models **1** and **2** of Calix[4]arene Conformers[a]

	cone	flattened cone	partial cone	1,2-alternate	1,3-alternate	chair
Structure **1**						
B3LYP/6-31G(d)						
E	−1081.46293	−1081.46520	−1081.46595	−1081.46285	−1081.46562	−1081.46492
ΔE	1.90	0.47	0.00	1.94	0.21	0.65
ΔE^{ZPE}	1.89	0.48	0.00	1.89	0.05	0.67
ΔH_{298}	1.29	0.48	0.00	0.76	0.11	0.68
ΔG_{298}	4.83	0.96	0.10	4.93	0.00	0.95
symmetry	C_{4v}	C_{2v}	C_s	C_1	C_{2v}	C_1
imaginary freq	−16.95	none	none	−20.6, −8.2	none	none
B3LYP/6-311+G(2d,2p)//B3LYP/6-31G(d)						
ΔE	1.14	0.39	0.00	1.66	0.19	0.39
MM3(92)[37]						
steric energy	0.0		1.2	1.8	1.7	
MM2[101]						
	0.0		0.67	1.51	0.82	2.66
Structure **2**						
BLYP/6-31G(d)						
ΔE[46]	0.0		10.7	18.6	18.1	
MM3(92)[37]						
steric energy	0.0		5.6	6.1	10.6	

[a] The absolute energies are reported in atomic units, and the relative and steric energies are given in kilocalories per mole.

correlation effects, which confirmed that cone **2** is indeed a minimum, unlike **1**. The breaking of the C_{4v} cone symmetry of substituted calix[4]arenes in the absence of hydroxyl groups, which results in the flattened cone conformation, has been attributed to electrostatic and steric interactions from substituent groups. In the case of the tetra-O-alkylated calix[4]arene "cone", temperature-dependent ^{1}H NMR[118] and computational[36,49] studies have shown that the observed cone conformation at room temperature is really the interconversion between the two flattened cone conformers. The computations presented here show for the first time that the aromatic core of the dehydroxylated calixarene contributes to a lowering from C_{4v} to C_{2v} symmetry.

(b) Partial Cone. In the absence of substituents, **1** prefers the partial cone conformation in the gas phase. Experimental evidence supports this conformational preference in the case of tetra-*O*-methylcalix[4]arene **6**, which lacks hydrogen-bonding stabilization. The partial cone often appears as the most stable conformer in a variety of alkylated calixarenes. This has been previously rationalized by electrostatics, steric repulsion, entropic control of conformational dynamics,[119] and a softer energy potential surface of the partial cone which counterbalances the steric hindrance by slight changes in its geometry.[36] Further evidence toward conformational stability can be provided by studies on solvation effects. The equilibrium favors the partial cone with decreasing solvent polarity,[32,120] which supports the idea that the partial cone is the preferred aromatic core conformation. Considering that the low dielectrics of nonpolar solvents are closer to a gas-phase environment, the contribution of the aromatic core to the conformational equilibrium must be considered.

(c) 1,3-Alternate. With only 0.21 kcal/mol separating the 1,3-alternate conformer from the partial cone, this conformer of **1** is very stable. This is interesting, since among the flexible substituted calix[4]arenes the 1,3-alternates are thought to be among the least stable. A previous DFT study revealed an 18.1 kcal/mol energy difference between the cone and the 1,3-alternate of **2**.[46] In the hydroxylated calix[4]arenes **2** and **3**, the most stable conformations are known to benefit from hydrogen bonding.[8] Clearly, the instability of the 1,3-alternate conformation in **2** or **3** does not arise from the aromatic core, rather from its inability to form stable hydrogen bonds. Consequently, the lack of hydrogen bonding and steric repulsion across the lower rim equally destabilizes all of the conformers in the dehydroxylated calixarene **1**, yielding conformations of approximately the same energy.

(d) 1,2-Alternate. Despite extensive searching, a stable minimum could not be located. The stability of this conformation in substituted calix[4]arenes is due mainly to hydrogen bonding. In *tert*-butylcalix[4]arene, NMR data revealed that after hydrogen substitution of two or three hydroxyls the molecule no longer adopted the 1,2-alternate conformer in solution.[37,42] Surprisingly, the X-ray structure of the tetradeoxy-*tert*-butylcalix[4]arene was observed in a 1,2-alternate conformation.[27] The computed instability of the 1,2-alternate aromatic core in the gas phase supports the notion that intermolecular packing interactions in the crystal influence the stability of this conformation in the solid phase, which has been previously suggested.[45]

(e) Chair. The chair is a true minimum in the gas phase with no imaginary frequencies and is one of the four more stable conformers. Although the chair is the conformation adopted by **1** in the X-ray structure of McMurry,[101] it is less stable than the partial cone, flattened cone, or 1,3-alternate according to the present results. According to McMurry, the chair, with one pair of rings lying in the same plane while the other two rings are perpendicular to that plane, exists because it maximizes $\pi-\pi$ stacking in the crystal and not because of its stability. Since this is not a common conformer of substituted calix[4]arenes and placement of the cations would be somewhat arbitrary,

(118) Ikeda, A.; Tsuzuki, H.; Shinkai, S. *J. Chem. Soc., Perkin Trans. 2* **1994**, 2073.
(119) Blixt, J.; Detellier, C. *J. Am. Chem. Soc.* **1994**, *116*, 11957.
(120) van Hoorn, W. P.; Briels, W. J.; van Duynhoven, J. P. M.; van Veggel, F.; Reinhoudt, D. N. *J. Org. Chem.* **1998**, *63*, 1299.

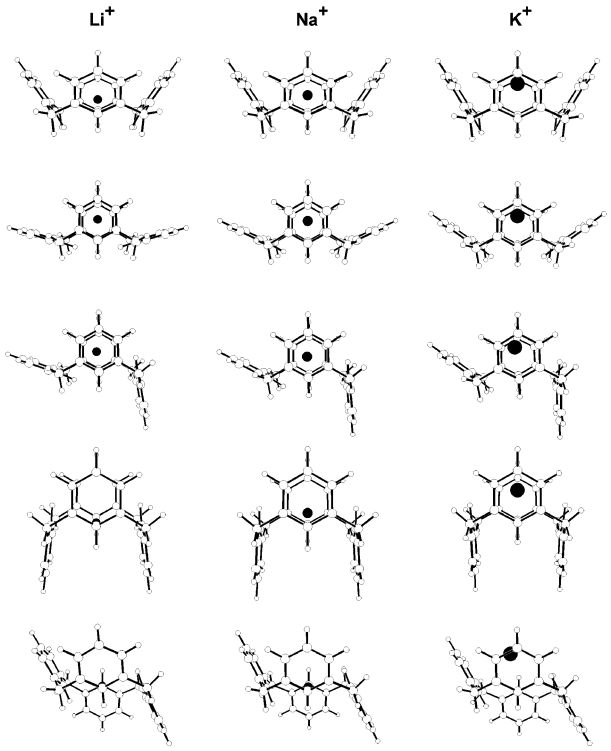

Figure 2. Geometry-optimized B3LYP/6-31G(d) conformers of **1** complexed with the alkali-metal cations. The cations are indicated by black spheres.

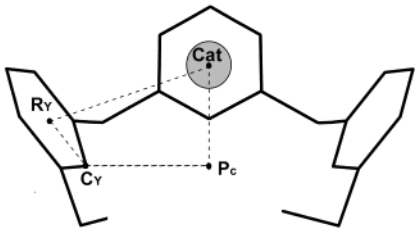

Figure 3. A schematic view of the calixarene core and geometric parameters used for analysis. P_c is the center of the reference plane containing the four methylene carbon bridges. R_Y is the centroid of a ring, where Y = A, B, C, or D.

complexation studies have not been carried out. Placement of the cation near ring B or D would result in a partial cone conformation due to repulsion between the cation and hydrogens. The distance between the two coplanar, electropositive hydrogens in the center of the DFT optimized chair is only 3.04 Å.

Structural Analysis of Conformers Complexed with Alkali Metals. The optimized complexes of the conformers with the alkali-metal cations are shown in Figure 2. Key structural changes for each conformer upon binding the cations are defined in Figure 3 and summarized in Table 3. The greatest variation occurs in the position of the rings, which bend inward toward the center (and the cation) when the $R_Y-C_Y-P_C$ angle decreases, and outward when the angle increases with respect to the uncomplexed conformer.

(a) Cone. C_{4v} complexes were optimized in which the cation was free to move along the C_4 principal axis. The imaginary frequencies observed in the parent conformer, which forced the cone to become a flattened cone, were still present. While the imaginary frequency of the uncomplexed cone was -17 cm^{-1}, the imaginary frequencies for the Li^+, Na^+, and K^+ complexes were -18.6, -18.9, and -25.3 cm^{-1}, respectively. Therefore, the C_{4v} complexes are transition structures, separating the complexes of the flattened cone. Surprisingly, the angle formed by the plane of the rings and the plane of the methylenes ($R_A-C_A-P_C$) decreases with increasing ionic radii upon complexation (by up to 5.6°). The greatest change occurs with K^+, where the distance between opposing ring centroids (R_A-R_C) changes from 6.89 to 6.74 Å. Li^+ complexation results in a contraction of the lower rim, where C_A-C_C changes from 5.23 to 5.18 Å, while the larger ionic radius of K^+ results in an expansion, from 5.23 to 5.30 Å. The ionic radii of Li^+, Na^+, and K^+ are 0.68, 0.97, and 1.33 Å, respectively,[121] which places the cations at different distances from the tighter, lower rim as reflected in the $Cat-P_C$ distances.

Table 3. Structural Changes of **1** upon Complexation[a]

	Cat–P_c	C_A–C_C	R_A–R_C	R_B–R_D	R_A–C_A–P_C	R_B–C_B–P_C
cone		5.234	6.893	6.893	126.9	126.9
Li^+−cone	0.721	*−0.058*	*−0.091*	*−0.091*	*−1.1*	*−1.1*
Na^+−cone	1.113	+0.014	*−0.092*	*−0.092*	*−2.8*	*−2.8*
K^+−cone	1.942	+0.068	*−0.151*	*−0.151*	*−5.6*	*−5.6*
flattened cone		5.188	5.507	7.869	98.3	162.9
Li^+−flattened cone	1.549	*−0.052*	*−0.852*	+0.129	*−16.1*	*−1.9*
Na^+−flattened cone	1.584	+0.006	*−0.386*	*−0.048*	*−6.1*	*−9.8*
K^+−flattened cone	2.073	+0.052	+0.374	*−0.325*	+6.5	*−18.0*
partial cone		5.148	5.535	7.063	99.8	163.9
Li^+−partial cone	1.410	*−0.034*	*−0.905*	+0.064	*−17.7*	*−7.3*
Na^+−partial cone	1.370	+0.040	*−0.379*	*−0.105*	*−8.6*	*−13.9*
K^+−partial cone	2.042	+0.048	+0.300	*−0.304*	+5.2	*−22.3*
1,3-alternate		5.066	5.715	5.715	105.5	105.5
Li^+−1,3-alternate	0.000	*−0.002*	*−0.302*	*−0.302*	*−5.8*	*−5.9*
Na^+−1,3-alternate	0.781	+0.230	*−0.560*	*−0.329*	*−16.3*	*−11.7*
K^+−1,3-alternate	1.865	+0.152	+0.075	*−0.589*	*−1.8*	*−17.1*

	Cat–P_c	C_A–C_C	R_A–R_B	R_B–R_C	R_A–C_A–P_C	R_B–C_B–P_C
1,2-alternate		5.145	4.743	7.098	124.5	124.5
Li^+−1,2-alternate	0.000	*−0.013*	*−0.086*	*−0.204*	*−6.3*	*−4.6*
Na^+−1,2-alternate	0.000	+0.148	*−0.060*	*−2.038*	*−10.9*	*−10.0*
K^+−1,2-alternate	2.479	*−0.022*	*−0.133*	*−2.078*	+4.2	+4.2

[a] Numbers in italics are the differences with respect to the uncomplexed conformers. Angles are reported in degrees and distances in angstroms.

(b) Flattened Cone. To eliminate the imaginary frequencies of the C_{4v} cone, complexes were optimized with C_{2v} symmetry, allowing cation movement along the C_2 axis. All C_{2v} complexes were found to be true minima by frequency analysis. The strong cation−π interaction with Li^+ causes rings A and C to move closer to each other and bend inward: R_A-R_C changes from 5.51 to 4.66 Å, and $R_A-C_A-P_C$ decreases from 98.3° to 82.2°. These changes are smaller in the complexation with Na^+, where the B and D rings move closer to Na^+, with a 9.8° decrease in the $R_B-C_B-P_C$ angle. The larger ionic radius of K^+ prevents rings A and C from bending inward; $R_A-C_A-P_C$ actually increases from 98.3° to 104.8°. However, rings B and D also move inward toward the cation, as demonstrated by the substantial decrease of 18° in the $R_B-C_B-P_C$ angle. Complexation with larger cationic radii causes the flattened cone conformer to change into a more conelike conformer.

(c) Partial Cone. Complexes involving the partial cone were optimized without symmetry restrictions. Rings A−C behave similarly as in the flattened cone. A and C bend inward to improve the cation−π interaction with Li^+ and Na^+, where the change in $R_A-C_A-P_C$ is −17.7° and −8.6°, but bend outward

(121) Kittel, C. *Introduction to Solid State Physics*, 7th ed.; Wiley: New York, 1996; p 78.

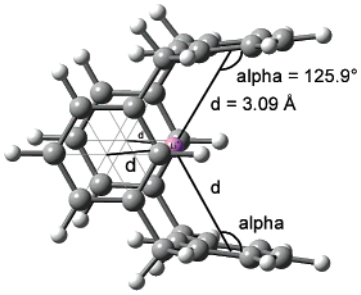

Figure 4. Detailed view of the 1,3-alternate conformer binding Li^+ cation.

to accommodate the larger K^+ radius, as shown by an $R_A-C_A-P_C$ change of $+5.2°$. With all three alkali metals, ring B bends inward toward the cation as demonstrated by decreasing $R_B-C_B-P_C$ values, with the greatest change occurring for K^+, as in the flattened cone complex. Figure 2 illustrates how the cation$-\pi$ interaction between the cations and ring B results in a slight displacement of the cations toward ring B, and away from the plane containing the centroids R_A, R_C, and P_C, in which they were placed at the beginning of the optimization.

(d) 1,3-Alternate. C_{2v} symmetry was used to optimize the 1,3-alternate complexes with the alkali-metal cations, which were verified as true minima. Surprisingly, Li^+ prefers to lie in the center of the reference plane defined by the methylene linkage carbons, $Cat-P_C = 0.0$ Å, where it is equidistant from the aromatic centroid of the four rings, as seen in Figure 4. $Cat-R_Y$ is 3.09 Å and $Cat-R_Y-C_Y$ is 54.1° for all four rings. Li^+ also causes a tightening of the complex in which all rings bend inward. To rule out other possible minima along the C_2 axis, a second unconstrained optimization was started with the Li^+ positioned between two rings at $Cat-P_C = 2.0$ Å, a geometry which seemed to optimize the cation$-\pi$ interaction with two of the rings. The C_1-optimized structure resulted in the same geometry as the C_{2v} conformer, with Li^+ at the center of the plane of the methylene carbons. In the complexes with Na^+ and K^+, the cations are 0.78 and 1.87 Å above the methylene plane, thus optimizing their placement between rings A and C, which was the behavior originally expected for Li^+. The positions of opposing ring pairs are correlated: when $R_A-C_A-P_C$ increases, $R_B-C_B-P_C$ decreases.

(e) 1,2-Alternate. Even though ground-state Li^+ and Na^+ complexes could not be located with the 1,2-alternate conformer using C_1 symmetry, the K^+ complex was found and determined to be a real minimum. The 1,2-alternate parent has two low-mode imaginary frequencies of -20.6 and -8.2 cm^{-1}, which disappear after complexation with only the K^+ cation. After the 1,2-alternate conformer complexes with Li^+, only the first imaginary frequency remains, and it is weaker at -11.9 cm^{-1}, while the complex with Na^+ still has two imaginary frequencies of -19.1 and -13.7 cm^{-1}. Both the Li^+ and Na^+ cations lie in the reference plane of the methylene carbons, while the larger K^+ moves 2.48 Å above the plane, interacting closely with adjacent rings A and B. Calculations with different starting geometries for the Li^+ and Na^+ resulted in the cations moving back into the methylene plane. The larger ionic size of K^+ prevents it from being inside the rim where four weak cation$-\pi$ interactions are better than two slightly stronger cation$-\pi$ interactions as revealed by the other complexes. Also, if the more electropositive Li^+ and Na^+ interact with adjacent faces then, they might induce a bending of these around the cations, which would strain the conformer. Indeed, K^+ complexation results in an outward movement of the two aromatic rings with which it interacts as indicated by the increase in the $R_A-C_A-P_C$ angle, thus eliminating the imaginary frequencies.

Energetic Analysis of the Conformations of Alkali-Metal Complexes. The cation selectivity of each conformer and the stability of the conformers complexed with a specific cation are two points of interest. The accuracy of B3LYP/6-31G(d) in computing cation$-\pi$ interactions must first be assessed. There are no gas-phase experimental binding data for **1**, but data are available for benzene, which is a well-known model for the cation$-\pi$ interaction.[55] Table 1 compares the present results to previous experimental and theoretical values. For the benzene−cation complexes, the B3LYP/6-31G(d) binding enthalpies ($\Delta H_{298}{}^b$) are in agreement with experimental binding enthalpies ($\Delta H_T{}^b$). The computed $\Delta H_{298}{}^b$ values for benzene interacting with Li^+, Na^+, and K^+ are -41.3, -27.8, and -18.1 kcal/mol, respectively. The computed values are within the experimental uncertainties of the $\Delta H_T{}^b$ values for Li^+ (-39.3 ± 3.2[75] and -37.9[115]), Na^+ (-28.0 ± 1.5,[113] but not -22.5 ± 1.5[75]), and K^+ (-17.1 ± 0.9[75] and -19.2[68]).

After the B3LYP accuracy was calibrated with experimental results on the 1:1 complex, the energies of the benzene−cation−benzene (2:1) complexes were compared with the recent CID data.[75] The computed ΔH^b value of -33.4 kcal/mol for benzene$-K^+-$benzene is within the experimental enthalpy error bars of the CID result at -34.0 ± 2.7 kcal/mol. Similar agreement with the benzene$-Li^+-$benzene binding enthalpy is computed at -67.8 kcal/mol, which falls within the -64.1 ± 4.9 kcal/mol CID range. It is not surprising that the computed enthalpy of binding of the 2:1 complex of benzene$-Na^+-$benzene is too strong at -49.6 kcal/mol when compared to the CID result of -41.7 ± 2.8 kcal/mol, since the computed B3LYP binding for the 1:1 complex was also stronger than the CID value. The overall similarity of these results with the 1:1 complexes suggests that, in the presence of more aromatic faces, B3LYP gives reliable results.

While for the 1:1 complexes with Li^+, Na^+, and K^+ the BSSE was 2.1, 1.8, and 1.9 kcal/mol, the 2:1 complexes had higher BSSEs of 3.2, 3.4, and 3.7 kcal/mol, respectively. These BSSE values are generally less than those obtained with the higher theory MP2. The BSSEs for the complexes between the conformations of **1** and K^+ are in the range of 1.5−2.8 kcal/mol, and if they are included, they do not change the ordering of the stability of the conformers.

Since the computed electronic binding energies are in excellent agreement with the experimental binding enthalpies, the ΔE^b will be discussed throughout this study. Inclusion of all corrections to the binding energies does not change a conformer's cation binding selectivity since the binding energies differ by at least 8 kcal/mol in all cases as reported in Table 4. ΔE^b was calculated by subtracting from the energy of the complex the energy of the cation and the energy of the conformer of **1** found in that complex. $\Delta E^{b,part}$ was obtained by subtracting from the energy of the complex the energy of the cation and the energy of the partial cone, which was the global minimum according to the electronic energies and enthalpies. $\Delta E^{b,part}$ includes the energy necessary for **1** to change from its most stable conformer into the conformer found in the complex, therefore providing information on the conformational stability

Table 4. Conformational Stability of the Complexes (ΔE) after Binding the Cations and Calculated Binding Energies (ΔE^{b}, $\Delta E^{b,part}$)[a]

		cone	flattened cone	partial cone	1,2-alternate	1,3-alternate
1−Li^+	E	−1088.84854	−1088.85940	−1088.86045	−1088.84596	−1088.86443
	ΔE	9.97	3.16	2.50	11.59	0.00
	ΔE^{b}	−63.42	−68.81	−69.02	−61.85	−71.70
	$\Delta E^{b,part}$	−61.55	−68.37	−69.02	−59.93	−71.52
1−Na^+	E	−1243.63145	−1243.63758	−1243.63827	−1243.62155	−1243.63916
	ΔE	4.84	0.99	0.56	11.05	0.00
	ΔE^{b}	−54.77	−57.20	−57.19	−48.61	−57.93
	$\Delta E^{b,part}$	−52.91	−56.75	−57.19	−46.70	−57.75
1−K^+	E	−1681.25667	−1681.25992	−1681.25814	−1681.24135	−1681.25440
	ΔE	2.03	0.0	1.11	11.65	3.46
	ΔE^{b}	−43.29	−43.90	−42.34	−33.73	−40.17
	$\Delta E^{b,cp}$	−40.50	−42.00	−39.70	−31.70	−38.7
	$\Delta E^{b,part}$	−41.42	−43.46	−42.34	−31.81	−39.99

[a] E is reported in atomic units, whereas ΔE, ΔE^{b}, and $\Delta E^{b,part}$ (defined in the text) are given in kilocalories per mole.

of the complexes. On the other hand, ΔE^{b} provides a measurement of cation complementarity[92,122] in cases of preorganized hosts. The cone and 1,2-alternate complexes are included for completeness, since they represent common conformations of substituted calix[4]arenes, but the presence of the imaginary frequencies rules out their existence as stable structures in the gas phase.

The gas-phase cation selectivities of the five conformers follow the electrostatic series $Li^+ > Na^+ > K^+$ in a similar manner to that of the benzene selectivity for the alkali-metal cations.[55] Complexation with Li^+ is preferred over that with Na^+ by at least 8 kcal/mol, and Na^+ complexation is preferred over that of K^+ by at least 11 kcal/mol. The stabilities of the conformers after complexing alkali-metal cations are given by the binding energies (ΔE^{b} and $\Delta E^{b,part}$), as reported in Table 4. The partial cone is no longer the lowest energy conformer. With Li^+ and Na^+, the 1,3-alternate forms the most stable complexes, while K^+ interacts most strongly with the flattened cone. According to ΔE^{b}, the two conformers most complementary to Li^+ are the 1,3-alternate and partial cone, while the flattened cone and cone offer greater complementary for the larger K^+ cation. Overall, the trends revealed by ΔE^{b} and $\Delta E^{b,part}$ are the same in this study, except in the less significant case of the cone and partial cone complexes with K^+. Although the partial cone binds K^+ more strongly by 0.92 kcal/mol, the cone has a greater complementarity for K^+ (1 kcal/mol) than the partial cone. ΔE^{b} and $\Delta E^{b,part}$ reveal that, among the stable structures (1,3-alternate, partial and flattened cone), complexation with Li^+ by the 1,3-alternate conformer is more stable by ca. 2.5 kcal/mol. Na^+ shows no strong binding preference for any of the three conformers, with binding energy differences within 1 kcal/mol of each other. Complexation of K^+ by the flattened cone is preferred by almost 3.5 kcal/mol over the complexation by the 1,3-alternate, but is only slightly more stable (within 1 kcal/mol) than the partial cone complex.

Deviation from Optimal Cation−π Geometries: Advantages of Multiple Interactions. A new and fundamental aspect of cation−π interactions is revealed by the geometries of these complexes. In an optimal cation−π interaction, the cation approaches the ring centroid along the normal to the carbon plane, where the quadrupole is strongest, with a Cat−R_Y−C_Y value of 90°.[55] If the aromatic carbon ring has electron-withdrawing or electron-donating substituents, the cation−π binding energies change accordingly, but the cation remains centered above the ring.[112] Exceptions occur when nitrogen or oxygen is part of the aromatic, altering the position of the quadrupole and resulting in a cation that is slightly off-center (∼0.2 Å).[85,86] Figure 5 illustrates the trajectories that the cations follow when moving within the Z−Y plane and the effect on the binding energies. Starting from the optimal position in which the cations lie along the normal axis (*Z*-axis) to the benzene, the angles between the cations and the normal were gradually increased while allowing the rest of the complex to optimize at B3LYP/6-31G(d). When Cat−R_Y−C_Y is 30°, the binding energies of Li^+, Na^+, and K^+ are still significant at 44%, 37%, and 26% of the binding energies when Cat−R_Y−C_Y is 90°.

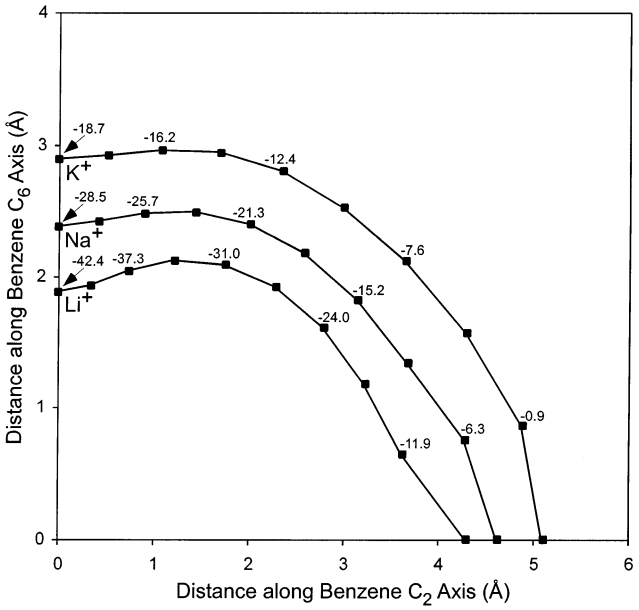

Figure 5. Cation paths around benzene obtained by increasing the angle of the cation to the C_6 ring normal. Data labels illustrate the decreasing binding energies (kcal/mol) of each geometry-optimized cation−benzene complex in which the angle was the only constraint. The origin of the axis is the benzene centroid.

Close inspection of distances and angles (Table 5) between the cations and the aromatic rings of **1** shows that they are far from the optimal cation−π angle parameters. Cation−benzene complexes were then optimized in which the Cat−R_Y−C_Y angles and the Cat−R_Y distances were constrained to equal the reported angles and distances found in the conformers of **1**. The cation−benzene complexes lack the attractive interactions with the remaining three rings present in **1**, the repulsive interactions between the aromatics, and the electron-donating effects of the

(122) Cram, D. J.; Lein, G. M. **1985**, *107*, 3657.

Table 5. Cation−π Interaction Parameters between the Conformers of **1** Complexed with Alkali-Metal Cations[a]

	ΔE^b	Cat–R_A	Cat–R_A–C_A	$\Delta E_A{}^b$	Cat–R_B	Cat–R_B–C_B	$\Delta E_B{}^b$	Cat–R_C	Cat–R_C–C_C	$\Delta E_C{}^b$	Cat–R_D	Cat–R_D–C	$\Delta E_D{}^b$
Li^+−cone	−63.4	3.425	47.4	*−23.1*	3.425	47.4	*−23.1*	3.425	47.4	*−23.1*	3.425	47.4	*−23.1*
Na^+−cone	−54.8	3.401	55.3	*−19.8*	3.401	55.3	*−19.8*	3.401	55.3	*−19.8*	3.401	55.3	*−19.8*
K^+−cone	−43.3	3.455	71.4	*−15.1*	3.455	71.4	*−15.1*	3.455	71.4	*−15.1*	3.455	71.4	*−15.1*
Li^+−flattened cone	−68.8	2.329	102.1	*−37.3*	4.194	34.2	*−13.1*	2.329	102.1	*−37.3*	4.194	34.2	*−13.1*
Na^+−flattened cone	−57.2	2.608	92.2	*−27.3*	4.044	40.6	*−13.7*	2.608	92.2	*−27.3*	4.044	40.6	*−13.7*
K^+−flattened cone	−43.9	3.014	89.3	*−18.4*	3.977	53.8	*−11.6*	3.014	89.3	*−18.4*	3.977	53.8	*−11.6*
Li^+−partial cone	−69.0	2.321	98.6	*−37.4*	3.986	36.2	*−15.7*	2.321	98.6	*−37.4*	4.174	38.5	*−13.3*
Na^+−partial cone	−57.2	2.583	88.3	*−27.5*	3.861	40.1	*−15.5*	2.583	88.3	*−27.5*	4.034	41.2	*−13.8*
K^+−partial cone	−42.3	2.988	88.4	*−18.5*	3.722	56.8	*−13.1*	2.998	88.4	*−18.5*	4.498	39.7	*−8.1*
Li^+−1,3-alternate	−71.7	3.085	54.1	*−27.5*	3.084	54.1	*−27.5*	3.085	54.1	*−27.5*	3.084	54.1	*−27.5*
Na^+−1,3-alternate	−57.9	2.671	77.7	*−26.4*	3.513	48.3	*−18.9*	2.671	77.7	*−26.4*	3.513	48.3	−18.9
K^+−1,3-alternate	−40.2	2.926	86.5	*−18.6*	4.205	41.1	*−9.7*	2.926	86.5	*−18.6*	4.205	41.1	*−9.7*
Li^+−1,2-alternate	−61.9	3.440	41.0	*−23.5*	3.462	39.8	*−23.2*	3.436	41.8	*−23.5*	3.444	41.6	*−23.4*
Na^+−1,2-alternate	−48.6	3.447	44.8	*−19.3*	3.462	44.1	*−19.1*	3.432	45.1	*−19.4*	3.447	44.4	*−19.3*
K^+−1,2-alternate	−33.7	2.996	85.7	*−18.2*	2.997	85.7	*−18.4*	5.642	31.5	*−3.0*	5.641	31.6	*−3.0*

[a] ΔE^b is the binding energy for complexes of **1**, while $\Delta E_A{}^b$, $\Delta E_B{}^b$, $\Delta E_C{}^b$, and $\Delta E_D{}^b$ correspond to the binding energy (in italics) of a cation−benzene complex in which the angle and distance equal those reported. Energies are reported in kilocalories per mole, distances in angstroms, and angles in degrees.

methylene linkages, but a qualitative assessment of the effect of variations in angles and distances on the energies can be made.

In the case of the lowest energy 1,3-alternate−Li^+ complex, the cation could interact strongly with two of the aromatic rings (A, C) at near right angles, but prefers to interact through four weaker cation−π bonds with the cation buried deep within the calixarene core. While the ΔE^b of the C_{6v} complex of Li^+−benzene in the gas phase is −42.4 kcal/mol at an optimal distance of 1.879 Å, the ΔE^b of a Li^+−benzene complex with a Cat−R_Y−C_Y of 54.1° and a Cat−R_Y distance of 3.085 Å is only −27.5 kcal/mol. Nevertheless, four of these weak interactions are more favorable than two optimal and two weak interactions: the ΔE^b of the D_{6h} benzene−Li^+−benzene complex is −69.7 kcal/mol (Table 1), while the ΔE^b of Li^+−1,3-alternate is −71.7 kcal/mol (Table 4). Na^+ and K^+ with their larger ionic radii are not centered on the 1,3-alternate methylene plane, but move upward to interact with two aromatic rings which then move closer to optimize the cation−π interactions. K^+ is almost normal to rings A and C (Cat−R_Y−C_Y = 86.6°) at a distance of 2.926 Å, which is close to the optimal K^+−benzene distance of 2.892 Å. Multiple cation−π interactions are shown to result from a balance of several factors including the cation's radius and the structural changes of the host. Each molecular conformation delivers a unique electrostatic potential, which is generated by a different number and combination of aromatic rings. However, the formation of multiple cation−π interactions depends on the nature of the cationic partner. For example, the resulting position of the cation in the 1,3-alternate and chair conformations, as shown in Figure 2, illustrates the importance of the cation, where the small and more electropositive Li^+ benefits from four weak cation−π interactions and the larger alkali-metal cations form two. Although previous experimental studies have suggested a role for multiple cation−π interactions, this is the first study quantifying the energetic advantages of these nonbonding motifs.

Conclusions

The energetic and structural preferences of a dehydroxylated calix[4]arene with and without alkali-metal cations are presented for the first time using density functional theory to isolate the effects of the aromatic core and cation−π interactions. The present results underscore the important contributions of weaker cation−π interactions to the overall binding strength in cases where multiple cation−π interactions are possible. Not only are multiple weak interactions equivalent to a single strong cation−π interaction in binding strength, but also the presence of several aromatic groups effectively controls the binding conformation. The computed effect is of interest not only in calix[4]arenes, but also in a wide variety of synthetic hosts and biochemical systems capable of multiple cation−π interactions.

Acknowledgment. We thank the Department of Defense (Grants DAAH04-96-1-0311 and DAAG55-98-1-0067), Department of Energy (Grants DE-FG26-01NT41287 and DE-FG26-02NT41556), National Energy and Technology Laboratory, IBM Corp., and Duquesne University (Faculty Development Award) for financial support to make this research possible.

Supporting Information Available: Density functional Cartesian coordinates, vibrational analysis, and computed thermochemical data of energy minima and transition structures (PDF). This material is available free of charge via the Internet at http://pubs.acs.org.

JA0285971